Iranian Polymer Journal
18 (4), 2009, 329-338

Available online at: http://journal.ippi.ac.ir

Non-isothermal Crystallization Kinetics of AB_3 Hyper-branched Polymer/Polypropylene Blends

Guangtian Liu* and Minshou Zhao

Institute of Environmental and Chemistry Engineering, Yanshan University
Qinhuangdao, 066004, Hebei Province, PR China

Received 29 October 2008; accepted 4 May 2009

ABSTRACT

The non-isothermal crystallization kinetics of pure polypropylene (PP) and AB_3 hyper-branched polymer (HBP)/PP blends (with 5% HBP content) were investigated with various cooling rates by differential scanning calorimetry (DSC) method. The Avrami analysis modified by Mandelkern and a method combined with Avrami and Ozawa equations were employed to describe the non-isothermal crystallization kinetics of the samples. The conclusion showed that at the same cooling rate, hyper-branched polymer could accelerate crystallization effectively. Furthermore, in the blends, the crystallization rate decreased when the higher molecular weight of HBP was added. An increase in the Avrami exponent showed that the addition of HBP influenced the mechanism of nucleation and the growth of PP crystallites. The possible reason and explanation could be attributed to the fractal structure of hyper-branched polymer which has an influence on the diffusion mode of crystallizable segments towards the growing nuclei. The polarized micrographs showed that the number of effective nuclei increased obviously in the HBP/PP blends where, HBP acts as a heterogeneous nucleation agent during the crystallization of the blends. In addition, the activation energy of crystallization was also obtained according to the Kissinger method and the results showed that the crystallization activation energy decreased remarkably in HBP/PP blends.

Key Words:

crystallization;
kinetics;
hyper-branched polymer;
blend;
polypropylene;
DSC.

(*) To whom correspondence to be addressed.
E-mail: lgtdesire@yahoo.com.cn

INTRODUCTION

It is known that the ultimate mechanical properties of the blends or composites based on crystallizable polymers are determined in part by crystallization behaviour of their components [1-3]. Polymer blends experience non-isothermal crystallization other than isothermal crystallization in industrial applications under processing and modeling; thus, an understanding of the non-isothermal crystallization behaviour is of technological and scientific importance. Generally, non-isothermal kinetics analysis is used to study the crystallization behaviour of crystalline polymers [4-11].

During the past decades, hyper-branched polymers have attracted considerable attention due to their remarkable properties such as reduction of melt and solution viscosity, high solubility, and ready to be functional in comparison to their linear analogues, resulting from the large number of reactive end-groups within a molecule of

approximately spherical molecular shape in the absence of chain entanglement [12-14]. Hyper-branched polymers are highly branched macromolecules with three-dimensional architecture. The general term of hyper-branched polymer includes both "perfectly-branched" dendrimers and "imperfectly branched" polymers. Typically, hyper-branched polymers comprise of a randomly branched structure, having precisely one focal unit and at least two branching points. Such polymers are generally prepared via AB_n-type monomers (where A is a functional group that reacts with B groups and $x \geq 2$) [15].

In recent years, many functional hyper-branched polymers with various terminal groups such as hydroxyl, carboxyl, acetoxy, and vinyl have been investigated as additives [16], catalysts [17], rheology modifiers [18], blend components [19], etc. The effect of adding hyper-branched polyester-amide to PP has been investigated and it is found that the dye-ability of PP fibres is highly improved without affecting other properties of the material [20]. Diao et al. [21] studied the effects of the addition of hyper-branched poly (amide-ester) grafted with polypropylene (PP-HBP) on the compatibility of PP/PVC blends.

The results showed that mechanical performance of the blend was enhanced. However, there has not been much work reported so far on the non-isothermal crystallization behaviour of hyper-branched polymer (HBP)/PP blend. In this paper, the non-isothermal crystallization kinetics of AB_3 HBP/PP blend (5% HBP content) is investigated using differential scanning calorimetry (DSC). Moreover, the reasons for the differences in crystallization behaviours of pure PP and HBP/PP blends are also given as well. This study would be useful for designing the processing parameters and obtaining the relationship between crystallization behaviour and the final mechanical properties of the blends.

EXPERIMENTAL

Materials

Commercial spherical i-PP granules (T30S) was provided by YanShan Petrochemical Co. Ltd. Different molecular weights of AB_3 HBP samples ($\overline{M}_n$ = 7800, 10820, and 12500 g/mol) were prepared [22], and the

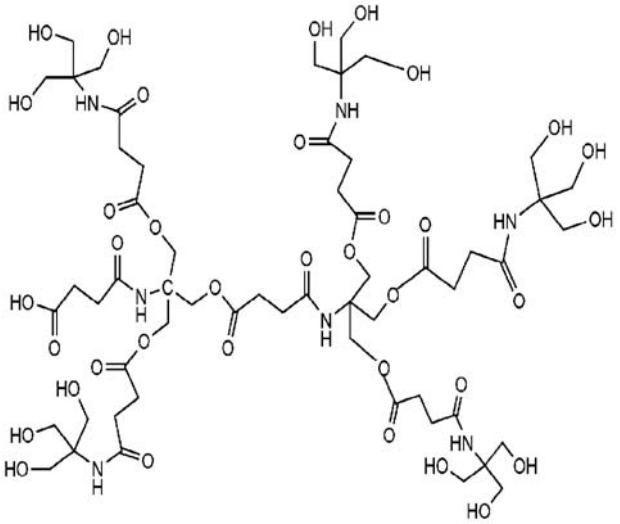

Figure 1. Schematic structures of AB_3 hyper-branched poly(amide-ester) (HBP).

schematic structures are shown in Figure 1. A sample of 5% HBP was blended with PP in a single-screw extruder (type XJ-20, Scientific Research Instrument Factory, Jilin University, Jilin, China). Before being extruded, HBP and PP were dried at 80°C for 4 h. The mixtures of HBP and PP at different ratios were extruded at 180°C under a screw rotating speed of 20 rpm. The extruded samples were cooled and then granulated.

Non-isothermal Crystallization Kinetics

The non-isothermal crystallization kinetics was investigated by using the Pyris6 Diamond type of a differential scanning calorimeter (DSC). Before the collection of data, all samples were heated to 200°C at a rate of 40°C/min and held in the molten state for 5 min to eliminate the influence of thermal history. All operations were carried out under a nitrogen environment. The weights of the samples were about 7 mg. Afterwards, the samples were cooled down to room temperature at a rate of 5°C/min, 10° C/min, 15°C/min, and 20°C/min, respectively.

Morphologies

The morphologies of the blends as thin films were studied by using an optical polarizing microscope (type 59-XA, Yongheng Optical Instrument Co., Shanghai, China) with a Mettler FP-90 automatic hot-stage thermal controller. The samples were sandwiched

between microscope coverslips and melted at 200°C for 5 min in a separate hot stage, and then rapidly moved to another hot stage which was equipped with the microscope and which was set to the crystallization temperature (130°C).

RESULTS AND DISCUSSION

From a technological point of view, the non-isothermal crystallization conditions approach more closely to the industrial conditions of polymer processing therefore, the study of crystallization of polymers under non-isothermal conditions is of great practical importance [23]. At the same time, because of more discrepancies in the crystallization rates of the samples at too high or too low crystallization temperatures, the isothermal measurement is often restricted to narrow temperature windows. Consequently, the non-isothermal crystallization is often conducted as a complementary approach to the isothermal data.

In this paper, the non-isothermal crystallization of PP and PP/HBP blends were investigated under different cooling rates. The exothermal curves of heat flow developing with temperature were recorded as shown in Figure 2. The parameters were taken from Figure 2 and shown in Table 1. As all the samples show similar types of the curves therefore, just one of the figures may be considered as a representative curve.

Table 1 shows that T_c of all samples drop with the increase of their respective cooling rates. The reason is that the molecular chains cannot enter crystal-grains when temperature is cooled too fast, and the polymers crystallize readily under supercooling temperature. Under the same cooling rate, the blends have higher T_c than PP and thus, the blends can crystallize at higher temperature. This means that the degree of supercooling required for crystallization is reduced because of the addition of HBP. Also ΔH_c is decreased with higher molecular weight of the HBP present in the blends, because HBP destroys the integrity of PP chains and decreases their activity and consequently leads to fewer crystallites in the blends.

The relative crystallinity at any crystallization temperature, C(t), can be taken from the ratio between integral area at temperature T and the whole crystallization area:

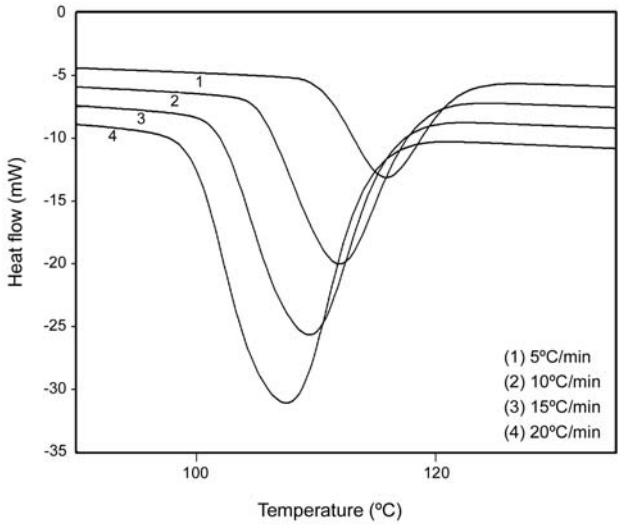

(a)

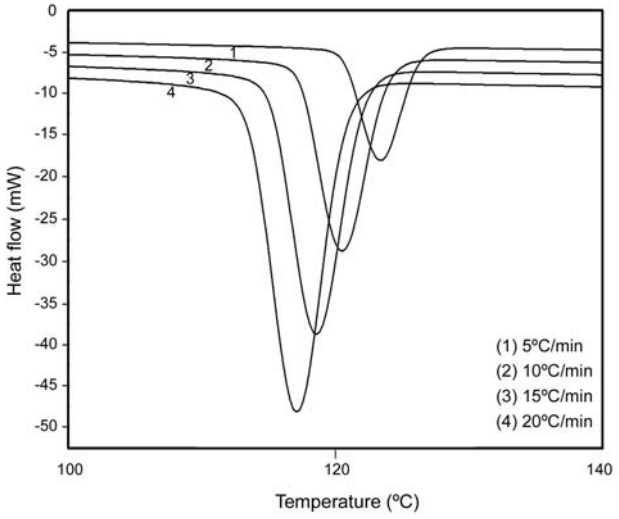

(b)

Figure 2. DSC cooling traces of: (a) iPP and (b) HBP/PP blend ($\overline{M}_{nHBP}$ = 7800 g/mol) recorded at different cooling rates.

$$C(t) = \int_{T_0}^{T} \left(\frac{dH_c}{dt}\right) dT \Big/ \int_{T_0}^{T_\infty} \left(\frac{dH_c}{dt}\right) dT \qquad (1)$$

where, T_0, T_∞, t, and dH_c are the crystallization onset temperature, the end crystallization temperature, the crystallization time, and the crystallization enthalpy at infinitesimal temperature dT, respectively.

Figure 3 shows the development of relative degree of crystallinity as a function of temperature for samples at various cooling rates. The plots of C(t) vs. T for PP are similar to those of the blends. It can be seen

Table 1. Avrami parameter of PP and HBP/PP blends from DSC non-isothermal crystallization exothermic peaks.

Samples (molecular weight of HBP, g/mol)	D (ºC/min)	n	Z_c	$t_{1/2}$ (min)	ΔH_c (J/g)	T_p (ºC)	R [a]
Pure PP	5	3.59	0.612	1.792	101.43	115.12	0.9995
	10	3.32	0.989	0.928	98.65	111.26	0.9996
	15	3.59	1.050	0.738	97.89	109.00	0.9999
	20	3.64	1.084	0.578	95.74	107.47	0.9999
$\overline{M}_n$ = 7800	5	5.26	0.718	1.279	82.23	123.41	0.9989
	10	5.86	1.076	0.828	81.76	120.43	0.9983
	15	5.14	1.212	0.531	80.87	118.55	0.9985
	20	5.65	1.219	0.465	81.09	117.21	0.9963
$\overline{M}_n$ = 10820	5	6.02	0.641	1.361	81.39	124.63	0.9987
	10	5.61	1.112	0.776	80.21	121.97	0.9989
	15	5.12	1.213	0.535	79.96	120.09	0.9989
	20	5.60	1.216	0.467	79.51	118.57	0.9972
$\overline{M}_n$ = 12500	5	6.32	0.631	1.358	81.54	123.89	0.9987
	10	6.03	1.094	0.810	80.59	120.82	0.9979
	15	4.97	1.212	0.542	80.45	118.84	0.9974
	20	4.82	1.214	0.468	79.23	117.24	0.9962

[a] correlation coefficient

that all these curves have the same inverse sigmoid shape, implying that only the lag effect of cooling rate on crystallization is observed. In Figure 3, at the same crystallinity, crystallization temperature decreases with increase in cooling rate. The reason is that molecular chains possess good fluidity and diffusability at lower cooling rate therefore, samples show higher crystallinity at higher temperature. Two different methods are used to discuss the non-isothermal crystallization kinetics in this paper.

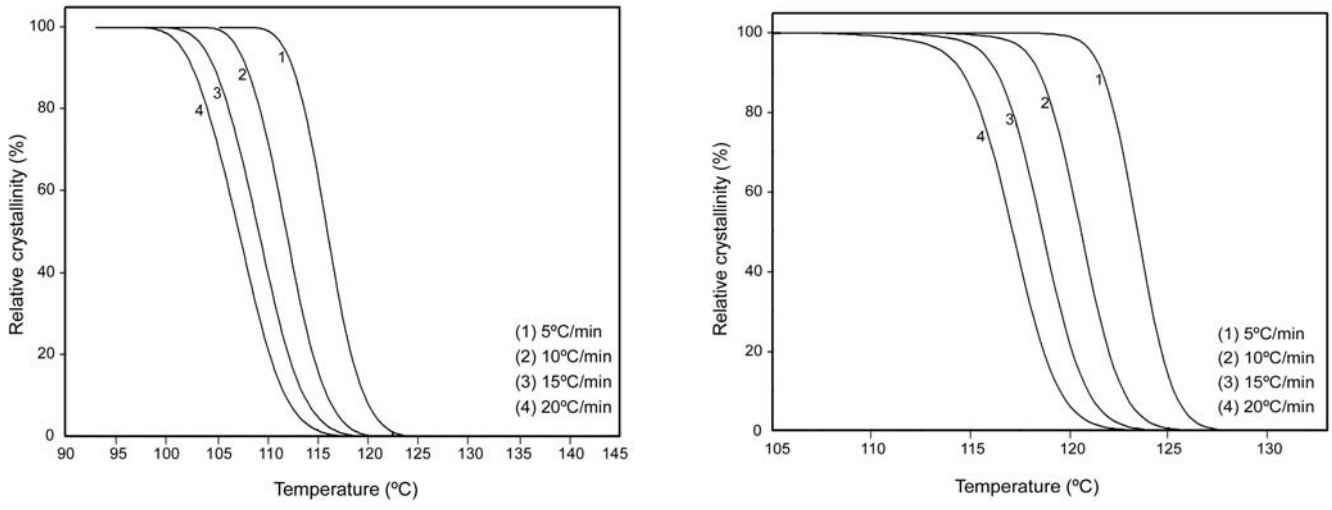

Figure 3. Development of relative crystallinity with temperature for non-isothermal crystallization of: (a) iPP and (b) HBP/PP blend ($\overline{M}_{nHBP}$ = 7800 g/mol).

Analysis of Non-isothermal Crystallization by Mandelkern Analysis Method

Mandelkern considered that the primary stage of non-isothermal crystallization could be described by the Avrami equation [24-27] which was based on the assumption that the crystallization temperature was constant. Mandelkern obtained the following equations:

$$1 - C(t) = \exp(-Z_t t^n) \quad (2)$$

$$\log\{-\ln[1 - C(t)]\} = n \log t + \log Z_t \quad (3)$$

where C(t), Zt, and n, are relative crystallinity at crystallization time t, the crystallization rate constant, and the Avrami exponent, respectively. Here, n represents the nucleation mechanism and growth dimension. Considering the character of non-isothermal crystallization, a new kinetic parameter, Z_c is introduced as follow:

$$\log Z_c = (\log Z_t) / D \quad (4)$$

where D is the cooling rate. According to eqn (3), plots of log [-ln (1-C(t))] vs. log t are shown in Figure 4 where, the good linearity of the plots verifies the advantage of the Mandelkern analysis method applied in this case. The parameters of n, Z_c and $t_{1/2}$ which are shown in Table 1 are obtained from Figure 4. The non-isothermal crystallization is a temperature-dependent process therefore, the Avrami exponent, n, does not have the same physical significance as in the isothermal crystallization. The former would be a summary value of n in the whole temperature range of the exothermic process. It is shown from Table1 that n values of PP vary from 3.32 to 3.64, and those of the blends range between 4.82 and 6.32. A notable increase in the Avrami exponent means the addition of HBP influences the mechanism of nucleation and the growth of PP crystallites. The possible reason is attributed to the fractal structure of hyper-branched polymer which has an influence on the diffusion mode of crystallizable segments towards the growing nuclei. The values of n are non-integer and the reason is that there are different crystallization mechanisms or hypo-crystallizations at the same time during non-isothermal crystallization. The larger the Z_c value, the higher would be the crystallization rate. At the same cooling rate, the much higher Z_c of the blends relative to PP indicates that HBP can prompt crystallization effectively. In that case, $t_{1/2}$ decreases with increasing cooling rate because of rapid freezing of chain mobility at high cooling rate. Furthermore, in the blends, the crystallization rate is found to decrease when the higher molecular weight of HBP is added.

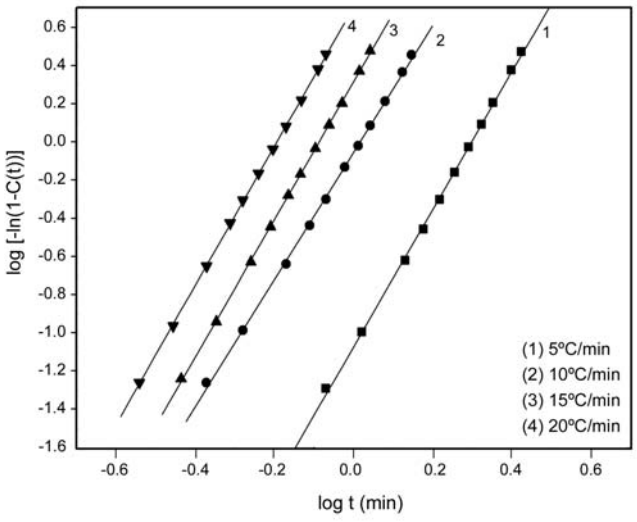

(a)

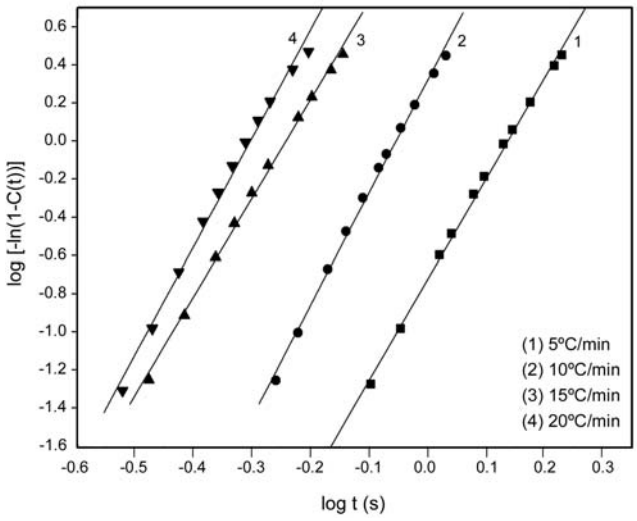

(b)

Figure 4. Plots of log [-ln(1-C(t))] as a function of log t for: (a) iPP and (b) HBP/PP blend ($\overline{M}_{nHBP}$ = 7800 g/mol) at different cooling rate.

Combined Avrami and Ozawa Equations

In order to find a method to describe exactly the non-

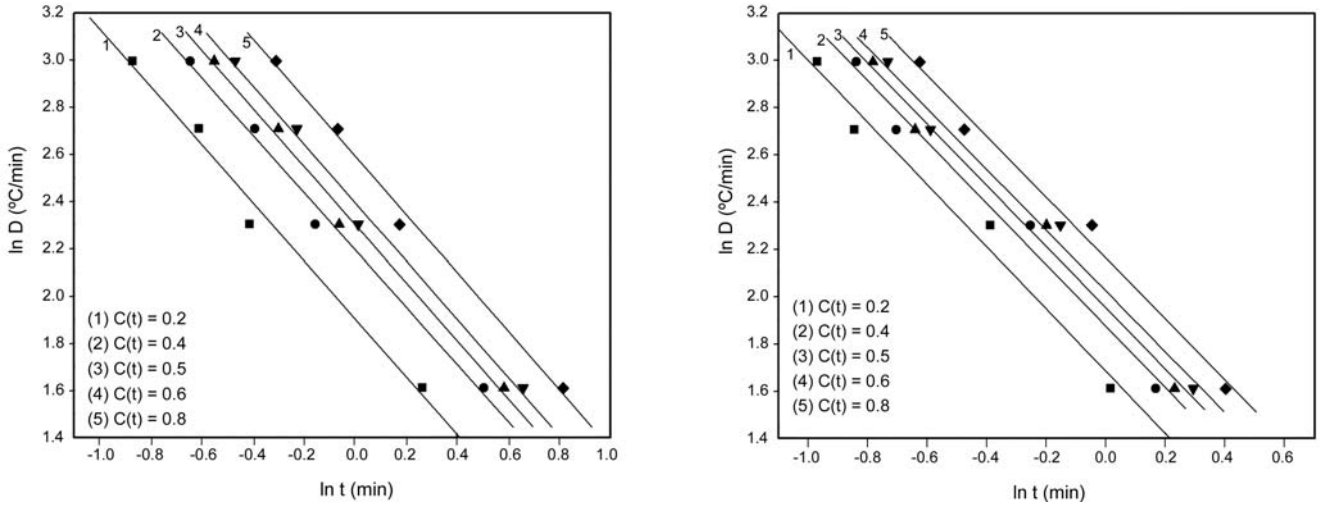

Figure 5. Plots of ln D vs. ln t for: (a) iPP and (b) HBP/PP blend ($\overline{M}_{nHBP}$ = 7800 g/mol).

isothermal crystallization process, Mo and co-workers [28] have proposed a different equation to study the non-isothermal crystallization by combining the Avrami and Ozawa equations, as the followings:

$$\ln Z_t + n \ln t = \ln K(T) - m \ln D \quad (5)$$

$$\ln D = 1/m \ln[K(T)/Z_t] - n/m \ln t \quad (6)$$

by defining α = n/m, the ratio between the Avrami and Ozawa exponents and $F(T)=[K(T)/Z_t]^{1/m}$, Mo et al. have obtained the following expression :

$$\ln D = \ln F(T) - \alpha \ln t \quad (7)$$

The parameter F(T) is the value of cooling rate which has to be chosen at unit crystallization time and when the measured system amounts to a certain degree of crystallinity. The smaller the value of F(T), the higher the crystallization rate becomes. Therefore, F(T) has a definite physical meaning.

At different relative crystallinities of samples (C(t) = 0.2, 0.4, 0.5, 0.6 and 0.8), the plots of ln D vs. ln t according to eqn (7) are shown in Figure 5. Using linearity fitting with these data, we can obtain a series of lines with -α as the slope and lnF(T) being the intercept. The values of α and F(T) are also listed in Table 2. At a certain relative crystallinity, a high value of F(T) means a high cooling rate needed to reach this C(t) in a unit time, which reflects the difficulty of its crystallization process. Table 2 shows that the value of F(T) increases with increasing relative crystallinity, indicating that at a given crystallization time, a higher cooling rate should be used to obtain a higher degree of crystallinity. However, at the same C(t), the values of F(T) for the blends are higher than that of the virgin PP, indicating that the crystallization rates of the formers are higher than that of the latter. In addition, in the blends, the variety trend of the crystallization rate is the same as the conclusion by Mandelkern analysis.

During the non-isothermal process, it is clear that HBP has a strong influence on the rate of crystallization. The crystallization rates of the blends are found to be higher when HBP was added, showing a rather rapid process of the non-isothermal crystallization. However, the crystallization rates of the blends decrease when the higher molecular weight of HBP was added. The possible explanation is that a large number of polar branched chains act as nucleation agent because of HBP introduction which promotes the nucleation. On the other hand, HBP may act as a lubricating agent due to the more or less spherical shape of the molecule and absence of chain entanglements which leads to a decrease in viscosity of the blends. The diffusion of crystallizable chain segments towards the growing nuclei is facilitated, and therefore the crystallization rate increases remarkably. In contrast, interactions such as hydrogen bonding between the polar groups of branching chains become

Table 2. Non-isothermal crystallization kinetics parameters from combination of Avrami-Ozawa equations.

Samples (molecular weight of HBP, g/mol)	C(t) (%)	α	F(T)	R [a]
Pure PP	20	1.230	6.719	0.9927
	40	1.214	8.989	0.9957
	50	1.232	10.004	0.9964
	60	1.236	10.979	0.9962
	80	1.239	13.397	0.9965
$\overline{M}_n$ = 7800	20	1.320	5.376	0.9891
	40	1.303	6.508	0.9911
	50	1.301	7.029	0.9922
	60	1.289	7.553	0.9934
	80	1.291	8.688	0.9941
$\overline{M}_n$ = 10820	20	1.221	5.663	0.9949
	40	1.229	6.760	0.9962
	50	1.238	7.185	0.9966
	60	1.240	7.652	0.9972
	80	1.269	8.688	0.9975
$\overline{M}_n$ = 12500	20	1.087	5.942	0.9944
	40	1.120	6.814	0.9965
	50	1.139	7.207	0.9969
	60	1.159	7.699	0.9972
	80	1.187	8.628	0.9976

[a] correlation coefficient

stronger with increasing molecular weight of HBP which give rise to a system of physically cross-linked network. Consequently, chain diffusion and mobility of the crystallizable segments diminish and thus, the crystallization process is emerged when the higher molecular weight of HBP is added.

Polarized Micrographs

Figure 6 shows the polarized micrographs of iPP and HBP/PP ($\overline{M}_{nHBP}$ = 12500 g/mol) blend at 130°C. The HBP/PP blend shows that clearly the number of effective nuclei increases, an indication that HBP has acted as a nucleating agent in the iPP phase and accelerated the nucleation and reduced the sphereulite size rapidly. This result also provides the evidence that crystallization of the blend proceeds mainly via heterogeneous nucleation.

Crystallization Activation Energy

Considering the influence of the various cooling rates, D, on the non-isothermal crystallization process, Kissinger proposed that the activation energy could be determined by calculating the variation of the crystallization peak with the cooling rate [29]. It reads:

$$\frac{d[\ln(D/T_P^2)]}{d(1/T_P)} = -\frac{\Delta E}{R} \quad (8)$$

where, R and T_p are the gas constant and the crystallization peak temperature. Graphs of $\ln(D/T_p^2)$ vs. $1/T_p$ are shown in Figure 7. The slope of the curve gives $-\Delta E/R$. Activation energy, ΔE, is calculated and shown in Table 3.

It can be seen in Table 3 that the activation energy

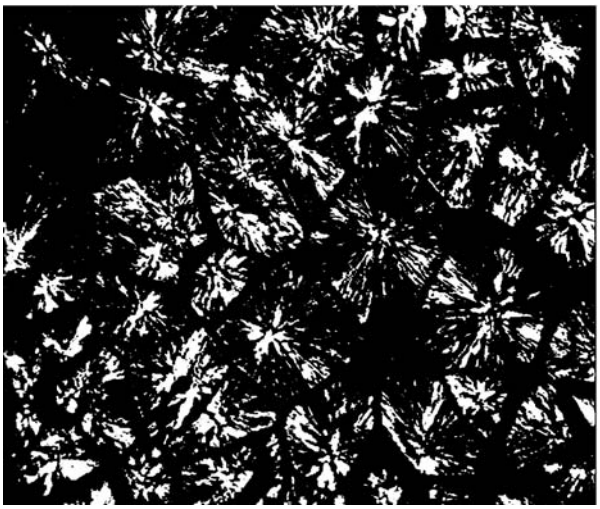

(a)

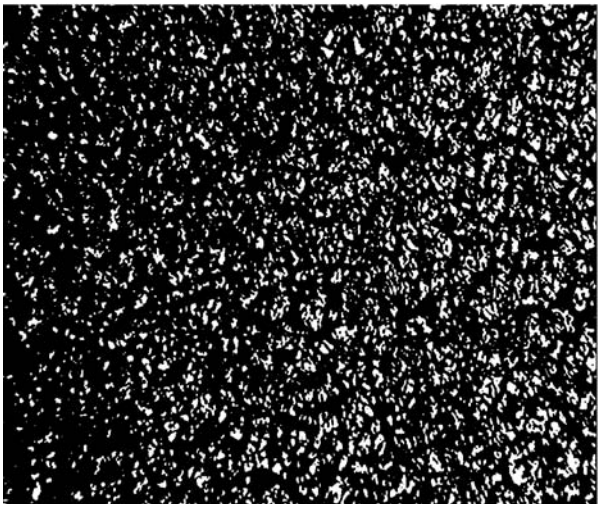

(b)

Figure 6. The polarized micrographs of: (a) iPP and (b) HBP/PP blend ($\overline{M}_{nHBP}$ = 12500 g/mol) at 130°C (magnification×100).

of HBP/PP is lower than that of pure PP. This shows that the blends crystallize more easily and HBP acts as a heterogeneous nucleating and lubricating agents which accelerate the crystallization. In addition, in the

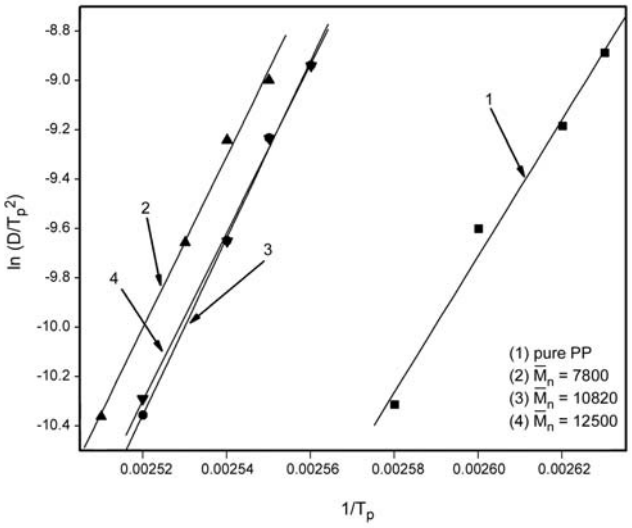

Figure 7. Kissinger plot for evaluating non-isothermal crystallization activation energy.

blends, activation energy becomes higher with the increasing molecular weight of HBP. The resulting issue is the same as the various trends of the crystallization rate.

CONCLUSION

In this paper, non-isothermal crystallization kinetics of HBP/PP blends using differential scanning calorimetry method was investigated. The Avrami and Mo's methods were employed to describe the non-isothermal crystallization process of PP and HBP/PP blends. The results have shown that a small addition of HBP in PP may affect the crystallization behaviour of PP. At the same cooling rate, HBP can prompt crystallization effectively. Furthermore, in the blends, the crystallization rate is decreased when the higher molecular weight of HBP is added. The addition of HBP with fractal structure influences the mechanism

Table 3. Activation energies of iPP and HBP/PP blends.

Samples / Calculated ΔE	iPP	$\overline{M}_n$ = 7800 (g/mol)	$\overline{M}_n$ = 10820 (g/mol)	$\overline{M}_n$ = 12500 (g/mol)
ΔE(KJ/mol)	-230.33	-298.99	-289.93	-284.05
R [a]	0.9934	0.9989	0.9972	0.9986

(a) correlation coefficient

of nucleation and the growth of PP crystallites. The crystallization activation energy has decreased remarkably in the HBP/PP blends. The polarized micrographs show that HBP acts as a heterogeneous nucleation agent during the crystallization of the blends.

REFERENCES

1. Avella M, Martuscelli E, Sellitti C, Garagnani E, Crystallization behaviour and mechanical properties of polypropylene based composites, *J Mater Sci*, **22**, 3185-3193, 1987.
2. Zhang ML, Liu YQ, Zhang XH, Gao JM, Huang F, Song ZH, Wei S, Qiao JL, The effect of elastomeric nano-particles on the mechanical properties and crystallization behavior of polypropylene, *Polymer*, **43**, 5133-5138, 2002.
3. Jose S, Aprem AS, Francis B, Chandy MC, Werner P, Alstaedt V, Thomas S , Phase morphology, crystallisation behaviour and mechanical properties of isotactic polypropylene/high density polyethylene blends, *Eur Polym J*, **40**, 2105-2115, 2004.
4. Li Z-M, Yang W, Li L-B, Xie B-H, Huang R, Yang MB, Morphology and nonisothermal crystallization of in situ microfibrillar poly(ethylene terephthalate)/polypropylene blend fabricated through slit-extrusion, hot-stretch quenching, *J Polym Sci B Polym Phys*, **42**, 374-385, 2004.
5. Yuan Q, Awate S, Misra RDK, Nonisothermal crystallization behavior of polypropylene-clay nanocomposites, *Eur Polym J*, **42**, 1994-2003, 2006.
6. Zhu XL, Wang CS, Wang B, Wang HP, Non-isothermal crystallization kinetics and nucleation activity of filler in polypropylene/microcrystalline cellulose composites, *Iran Polym J*, **17**, 297-309, 2008.
7. Dobreva T, Lopez-Majada JM, Perena JM, Perez E, Benavente R, Nonisothermal melt-crystallization kinetics of isotactic polypropylene synthesized with a metallocene catalyst and compounded with different quantities of an a nucleator, *J Appl Polym Sci*, **109**, 1338-1349, 2008.
8. Wang JB, Dou Q, Nonisothermal crystallization kinetics and melting behaviors of isotactic polypropylene/N,N′,N″-tris-tert-butyl-1,3,5-benzene-tricarboxamide, *J Macromol Sci B Phys*, **47**, 629-642, 2008.
9. Wang JB, Dou Q, Non-isothermal crystallization kinetics and morphology of isotactic polypropylene (iPP) nucleated with rosin-based nucleating agents, *J Macromol Sci B Phys*, **46**, 987-1001, 2007.
10. Tao Y, Pan Y, Zhang Z, Mai K, Non-isothermal crystallization, melting behavior and polymorphism of polypropylene in -nucleated polypropylene/recycled poly (ethylene terephthalate) blends, *Eur Polym J*, **44**, 1165-1174, 2008.
11. Hong H, He H, Jia D, Hua B, Lin G, Influence of adjustable grafted side Chains on the non-isothermal crystallisation of a ternary-monomer solid phase graft copolymer of polypropylene, *Polym Polym Compos*, **16**, 131-138, 2008.
12. Nunez CM, Chiou B-S, Andrady AL , Khan SA, Solution rheology of hyperbranched polyesters and their blends with linear polymers, *Macromolecules*, **33**, 1720-1726, 2000.
13. Voit BI, New developments in hyperbranched polymers, *J Polym Sci A Polym Chem*, **38**, 2505-2525, 2000.
14. Voit BI, Hyperbranched polymers: a chance and a challenge, *C R Chim*, **6**, 821-832, 2003.
15. Jikei M, Kakimoto M-A, Hyperbranched polymers: a promising new class of materials, *Prog Polym Sci*, **26**, 1233-1285, 2001.
16. Orlicki JA, Moore JS, Sendijarevic I, McHugh AJ, Role of end-group functionality on the surface segregation properties of HBPs in blends with polystyrene: application of HBPs as dewetting inhibitors, *Langmuir*, **18**, 9985-9989, 2002.
17. Slagt MQ , Stiriba S-E , Kautz H, Gebbink RJMK, Frey H, van Koten G, Optically active hyperbranched polyglycerol as scaffold for covalent and noncovalent immobilization of platinum(II) NCN-pincer complexes, catalytic application and recovery, *Organometallics*, **23**, 1525-1532, 2004.
18. Hong Y, Coombs SJ , Cooper-White JJ , Mackay ME , Hawker CJ, Malmstrom E, Rehnberg N, Film blowing of linear low-density polyethylene blended with a novel hyperbranched polymer processing aid, *Polymer*, **41**, 7705-7713, 2000.
19. Schmaljohann D, Potschke P, Hassler R, Voit BI,

Froehling PE, Mostert B, Loontjens JA, Blends of amphiphilic, hyperbranched polyesters and different polyolefins, *Macromolecules*, **32**, 6333-6339, 1999.
20. Burkinshaw SM, Froehling PE , Mignanelli M, The effect of hyperbranched polymers on the dyeing of polypropylene fibres, *Dyes Pigments*, **53**, 229-235, 2002.
21. Wang SJ, Ba XW, Zhao BH, Zhang SW, Hou WL, Synthesis and polymerization kinetics of AB_3 type hyperbranched poly(anide-ester)s, *Acta Polym Sin*, **5**, 634-639, 2004.
22. Diao JZ, Ba XW, Ding HT, Niu JT, Effect of hyperbranched poly(amide-ester) grafted polypropylene on the compatibility of polypropylene/poly(vinyl chloride) blends, *Iran Polym J*, **14**, 287-293,2005.
23. Di Lorenzo ML, Silvestre C, Non-isothermal crystallization of polymers, *Prog Polym Sci*, **24**, 917-950, 1999.
24. Mandelkern L, *Crystallization of Polymers*, McGraw Hill, New York, 1964.
25. Avrami M, Kinetics of phase change. I: general theory, *J Chem Phys*, **7**, 1103-1112, 1939.
26. Avrami M, Granulation, phase change, and microstruc-ture kinetics of phase change. III, *J Chem Phys*, **9**, 117-184, 1941.
27. Grenier D, Prud'homme RE, Avrami analysis: three experimental limiting factors, *J Polym Sci Polym Phys Ed*, **18**, 1655-1657, 1980.
28. Liu TX, Mo ZS, Wang SE, Zhang HE, Nonisothermal melt and cold crystallization kinetics of poly(aryl ether ether ketone), *Polym Eng Sci*, **37**, 568-573, 1997.
29. Kissinger HE , Variation of peak temperature with heating rate in differential thermal analysis, *J Res Natl Bur Stand*, **57**, 217-221, 1956.